Available online at www.sciencedirect.com

ScienceDirect

IFAC Papers Online CONFERENCE PAPER ARCHIVE

IFAC PapersOnLine 52-16 (2019) 31–35

Non-linear analysis of a modified QPSK Costas loop ⋆

N.V. Kuznetsov *,**,*** **M.V. Blagov** *,** **E.V. Kudryashova** *
J. Ladvanszky **** **M.V. Yuldashev** * **R.V. Yuldashev** *

* *Faculty of Mathematics and Mechanics, Saint-Petersburg State University, Russia (e-mail: nkuznetsov239@gmail.com).*
** *Dept. of Mathematical Information Technology, University of Jyväskylä, Finland*
*** *Institute for Problems in Mechanical Engineering RAS, Russia*
**** *Ericsson Telecom, Hungary*

Abstract: A Costas loop is one of the classical phase-locked loop based circuits, which demodulates data and recovers carrier from the input signal. The Costas loop is essentially a nonlinear control system and its nonlinear analysis is a challenging task. In this article for a modified QPSK Costas loop we analyze the hold-in, pull-in and lock-in ranges. New procedure for estimation of the lock-in range is considered and compared with previously known approach.

Keywords: Costas loop, PLL, non-linear analysis, PSK demodulator, numerical simulation, lock-in range

1. INTRODUCTION

The Costas loop is a modification of the phase-locked loop circuit (Viterbi, 1966; Matrosov et al., 2013; Best, 2007; Kolumban, 2015; Best, 2018; Ladvánszky, 2018), which demodulates data and recovers carrier from the input signal. Here we study a modified QPSK Costas loop for 4-phase-shift keying (PSK) demodulation (4 phases are used for modulation) based on the folding operation Ladvánszky and Covács (2018). Phase-shift keying (is a digital modulation process which conveys data by changing (modulating) the phase of a reference signal (the carrier wave), the modulation occurs by varying the phase of sine and cosine inputs at a precise time.

The Costas loop is essentially a nonlinear control system and its nonlinear analysis is a challenging task. We derive a mathematical nonlinear model (so-called baseband model) of the modified QPSK Costas loop and analyze the hold-in, pull-in and lock-in ranges by using a combination of classical linear methods, phase-plane analysis and numerical methods.

2. MATHEMATICAL MODEL

Consider the modification of the Quadrature-Phase Shift Keying Costas loop proposed in (Ladvánszky and Covács, 2018) (see Fig. 1). It is convenient to consider input QPSK signal in the following form

$$\sqrt{2}\sin(\theta_{\text{ref}}(t)+\tfrac{n(t)\pi}{4}),\quad \theta_{\text{ref}}(t)=\omega_{\text{ref}}t,\quad n(t)\in\{1,3,5,7\}.$$

Here $\dot\theta_{\text{ref}}(t)=\omega_{\text{ref}}$ denotes carrier frequency and $n(t)$ corresponds to digital data (two bits per symbol), $\theta_{\text{ref}}(t)$ is a reference phase [1].

The input signal is multiplied by inphase and quadrature phase VCO outputs $\sqrt{2}\cos(\theta_{\text{vco}}(t))$ and $\sqrt{2}\sin(\theta_{\text{vco}}(t))$, with $\theta_{\text{vco}}(t)$ being the phase of VCO. The resulting signals are

$$\begin{aligned} v_I(t) &= \sin(\theta_{\text{ref}}(t)+\tfrac{n(t)\pi}{4}-\theta_{\text{vco}}(t))+\\ &+\sin(\theta_{\text{ref}}(t)+\tfrac{n(t)\pi}{4}+\theta_{\text{vco}}(t)),\\ v_Q(t) &= \cos(\theta_{\text{ref}}(t)+\tfrac{n(t)\pi}{4}-\theta_{\text{vco}}(t))-\\ &-\cos(\theta_{\text{ref}}(t)+\tfrac{n(t)\pi}{4}+\theta_{\text{vco}}(t)) \end{aligned}$$

Here, from an engineering point of view, the high-frequency terms $\cos(\theta_{\text{ref}}(t)+\theta_{\text{vco}}(t)+\frac{n(t)\pi}{4})$ and $\sin(\theta_{\text{ref}}(t)+\theta_{\text{vco}}(t)+\frac{n(t)\pi}{4})$ are removed by low-pass filters LPF 1 and LPF 2 [2]. Thus, the signals $Q(t)$ and $I(t)$ on the upper and lower branches can be approximated as

$$\begin{aligned} &Q(t)\approx\sin(\theta_e(t)+\tfrac{n(t)\pi}{4}),\quad I(t)\approx\cos(\theta_e(t)+\tfrac{n(t)\pi}{4}),\\ &\theta_e(t)=\theta_{\text{ref}}(t)-\theta_{\text{vco}}(t). \end{aligned} \tag{1}$$

Blocks which take absolute values have the following outputs:

⋆ We acknowledge support from Russian Science Foundation project 19-41-02002 .

[1] Coefficient $\sqrt{2}$ is can be omitted or replaced by another coefficient, representing signal power.

[2] While this is reasonable from a practical point of view, its use in the analysis of Costas loop requires further consideration (see, e.g., (Piqueira and Monteiro, 2003)). The application of averaging methods allows one to justify the Assumption and obtain the conditions under which it can be used (see, e.g., (Kuznetsov et al., 2017a)).

10.1016/j.ifacol.2019.11.751

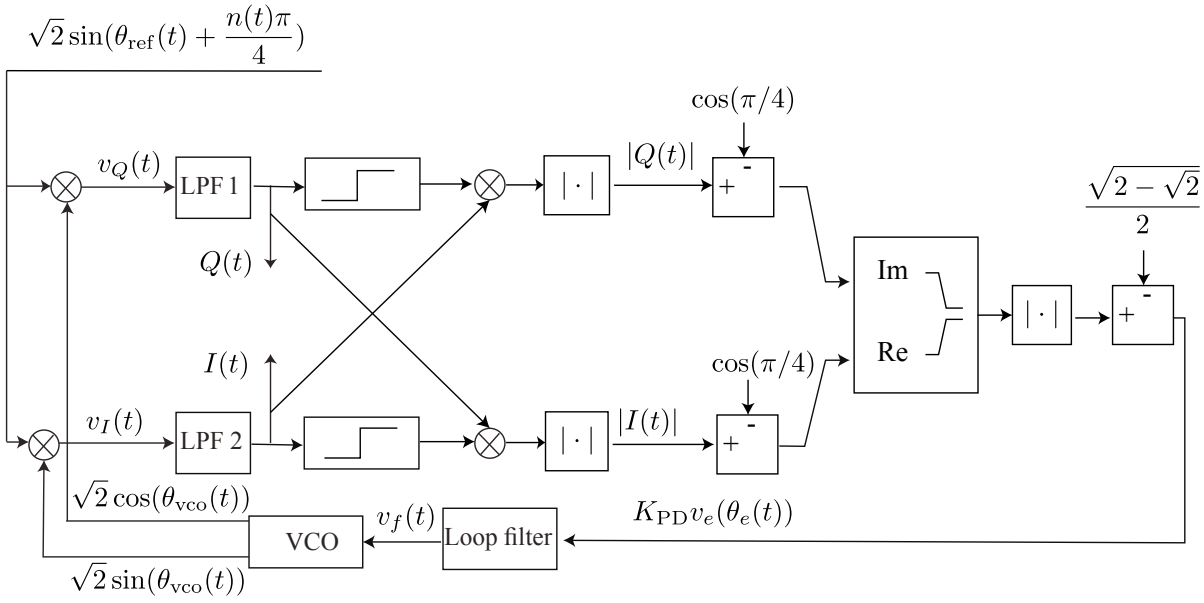

Fig. 1. Modified QPSK Costas loop proposed in (Ladvánszky and Covács, 2018).

$$
\begin{aligned}
&|\sin(\theta_e(t)+\frac{n(t)\pi}{4})\text{sign}\cos(\theta_e(t)+\frac{n(t)\pi}{4})|=\\
&=|\sin(\theta_e(t)+\frac{n(t)\pi}{4})|=|Q(t)|,\\
&|\cos(\theta_e(t)+\frac{n(t)\pi}{4})\text{sign}\sin(\theta_e(t)+\frac{n(t)\pi}{4})|=\\
&=|\cos(\theta_e(t)+\frac{n(t)\pi}{4})|=|I(t)|,
\end{aligned}
\tag{2}
$$

These signals are shifted by $-\cos(\frac{\pi}{4})$ and combined by **Re Im** block to complex signal

$$
|\cos(\theta_e(t)+\tfrac{\pi}{4})|-\cos(\tfrac{\pi}{4})+j(|\sin(\theta_e(t)+\tfrac{\pi}{4})|-\sin(\tfrac{\pi}{4})).
\tag{3}
$$

Then absolute value of complex signal is centered

$$
K_{\rm PD}v_e(\theta_e(t))=
$$

$$
\sqrt{2-\sqrt{2}(|\sin(\theta_e(t)+\tfrac{\pi}{4})|+|\cos(\theta_e(t)+\tfrac{\pi}{4})|)}-\frac{\sqrt{2-\sqrt{2}}}{2},
\tag{4}
$$

Here amplitude of (4) is $K_{\rm pd}=\frac{\sqrt{2-\sqrt{2}}}{2}$ and $v_e(\theta_e)$ is normalized phase detector characteristic with unit amplitude[3]. Note, that (4) is $\frac{\pi}{2}$–periodic, thus independent of modulated data $n(t)$. This allows to track changing reference frequency during the data demodulation. The PD characteristics (4) can be approximated with triangular waveform (see Fig. 2):

$$
v_e(\theta_e)\approx\begin{cases}
\frac{4}{\pi}\theta_e-\frac{\pi}{2}n,\\
\quad\text{if } \frac{\pi}{2}n\le\theta_e(t)\le\frac{\pi}{2}n+\frac{\pi}{4},\\
-\frac{4}{\pi}\theta_e+2-\frac{\pi}{2}n,\\
\quad\text{if } \frac{\pi}{2}n+\frac{\pi}{4}\le\theta_e(t)\le\frac{\pi}{2}(n+1),
\end{cases}
\tag{5}
$$

[3] Alternatively Atomatic Gain Controll (AGC) circuits can be used to keep desired signal centered. AGC allows to make the loop less sensitive to variations of input signal amplitudes and does not change the mathematical model.

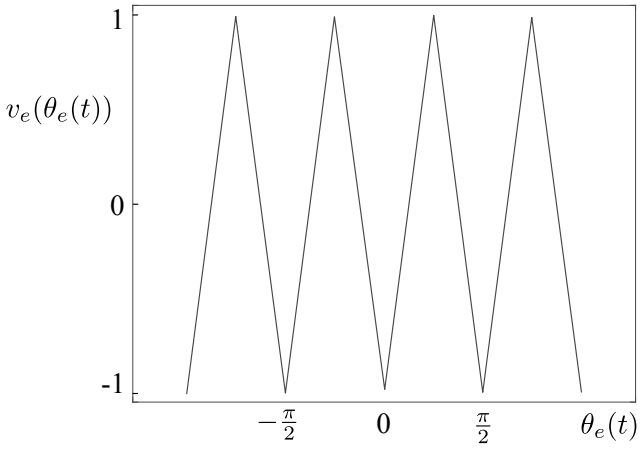

Fig. 2. Phase detector characteristic

where $n\in\mathbb{Z}$.

The relationship between the input $v_e(\theta_e(t))$ and the output $v_f(t)$ for the Loop filter with transfer function

$$
H(s)=\frac{1+\tau_2 s}{\tau_1 s},\quad \tau_1>0,\quad \tau_2>0,
\tag{6}
$$

is

$$
\begin{aligned}
\dot{x}(t)&=\frac{1}{\tau_1}K_{\rm PD}v_e(\theta_e(t)),\\
v_f(t)&=x(t)+\frac{\tau_2}{\tau_1}K_{\rm PD}v_e(\theta_e(t)),
\end{aligned}
\tag{7}
$$

where $x(t)$ is the filter state.

The control signal $v_f(t)$ adjusts the VCO frequency:

$$
\dot{\theta}_{\rm vco}(t)=\omega_{\rm vco}(t)=\omega_{\rm vco}^{\rm free}+K_{\rm vco}v_f(t),
\tag{8}
$$

where $\omega_{\rm vco}^{\rm free}$ is the VCO free-running frequency and $K_{\rm vco}>0$ is the VCO gain. Nonlinear VCO models can be similarly considered, see, e.g. (Margaris, 2004; Suarez, 2009; Bonnin et al., 2014; Bianchi et al., 2016). The frequency of the

input signal (also called as a reference frequency) is usually assumed to be constant (see, e.g. (Gardner, 1966)):

$$\dot{\theta}_{\rm ref}(t) = \omega_{\rm ref}(t) \equiv \omega_{\rm ref}. \tag{9}$$

The difference between the reference frequency and the VCO free-running frequency is denoted as $\omega_e^{\rm free}$:

$$\omega_e^{\rm free} \equiv \omega_{\rm ref} - \omega_{\rm vco}^{\rm free}. \tag{10}$$

Combining equations (7)–(10) one obtains a nonlinear baseband model (*nonlinear mathematical model in the signal's phase space*, i.e. in the state space: the filter's state x and the difference between the signal's phases θ_e):

$$\begin{aligned} \dot{x}(t) &= \frac{1}{\tau_1} K_{\rm PD} v_e(\theta_e(t)), \\ \dot{\theta}_e &= \omega_e^{\rm free} - K_{\rm vco}\left(x(t) + \frac{\tau_2}{\tau_1} K_{\rm PD} v_e(\theta_e(t))\right). \end{aligned} \tag{11}$$

Further without loss of generality we consider $K_{\rm PD} = 1$ (x and $K_{\rm vco}$ can be re-scaled: $x \to K_{\rm PD}x$, $K_{\rm PD}K_{\rm VCO} \to K_{\rm VCO}$). Initial state of the loop consists of $\theta_e(0)$ (initial phase shift of the VCO signal with respect to the reference signal) and $x(0)$ (initial state of the Loop filter).

Note, that (11) is not changed under the transformation

$$\big(\omega_e^{\rm free}, x(t), \theta_e(t)\big) \to \big(-\omega_e^{\rm free}, -x(t), -\theta_e(t)\big). \tag{12}$$

This allows to study system (11) for $\omega_e^{\rm free} > 0$ only and introduce the concept of *frequency deviation* (or *frequency offset*):

$$|\omega_e^{\rm free}| = |\omega_{\rm ref} - \omega_{\rm vco}^{\rm free}|. \tag{13}$$

Frequency deviation is used to define stability ranges of the circuit (pull-in, hold-in, and lock-in).

3. LOCAL STABILITY ANALYSIS

For a nonlinear baseband model (11) one can consider conditions of complete synchronization [4], i.e. the frequency error is zero and the phase difference $\theta_e(t)$ is constant:

$$\dot{\theta}_e(t) \equiv 0, \quad \theta_e(t) \equiv \theta_{eq}.$$

For the second equation of (11) the above equations implies that the loop filter state is also constant:

$$x(t) \equiv x_{eq}, \ \dot{x}(t) \equiv 0.$$

Thus, the locked states of the baseband model are given by the equilibria of the system (11). Equilibria can be found from the relations

$$\begin{aligned} \frac{1}{\tau_1} v_e(\theta_{eq}) &= 0, \\ \omega_e^{\rm free} - K_{\rm vco} x_{eq} &= 0. \end{aligned}$$

For any $\omega_e^{\rm free}$ the equilibria

$$\big(\theta_{eq}^s, x_{eq}\big) = \left(\frac{\pi}{2}n + \frac{\pi}{4}, \frac{\omega_e^{\rm free}}{K_{\rm vco}}\right), \quad n \in \mathbb{Z},$$

are stable. The remaining equilibria

$$\big(\theta_{eq}^u, x_{eq}\big) = \left(\frac{\pi}{2}n - \frac{\pi}{4}, \frac{\omega_e^{\rm free}}{K_{\rm vco}}\right), \quad n \in \mathbb{Z},$$

are unstable (saddle equilibria) [5] Since stable equilibria exists independently of $\omega_e^{\rm free}$, the hold-in range is infinite.

4. THE LOCK-IN RANGE

Frequency deviations for which the baseband model (11) achieves a locked state for any arbitrary initial state ($x(0)$, $\theta_e(0)$) correspond to the *pull-in range* $[0, \omega_p)$ (see, e.g., (Kuznetsov et al., 2015; Leonov et al., 2015)). For the model (11) it can be shown using Lyapunov functions, that its pull-in range is infinite (Alexandrov et al., 2015).

However, VCO frequency $\omega_{\rm vco}(t)$ may be slowly tuned to the carrier frequency $\omega_{\rm ref}$, and the phase error $\theta_e(t)$ may substantially increase during the acquisition process. To describe this effect rigorously, the notion of cycle slipping is used (see, e.g., (Ascheid and Meyr, 1982; Ershova and Leonov, 1983)): if $\limsup_{t\to+\infty} |\theta_e(0) - \theta_e(t)| \geq \pi$ then it is said that cycle slipping occurs.

Definition 1. (Kuznetsov et al., 2015; Leonov et al., 2015; Best et al., 2016) The lock-in range is a largest interval of frequency deviations $\left|\omega_e^{\rm free}\right| \in [0, \omega_l)$ inside the pull-in range, such that after an abrupt change of $\omega_e^{\rm free}$ within the lock-in range the PLL reacquires lock, if it is not interrupted, without cycle slipping. The frequency deviation ω_l is called a *lock-in frequency*.

Consider a practical way to estimate ω_l for the model (11) (Leonov et al., 2015; Kuznetsov et al., 2017b). Without loss of generality we fix $\omega_{\rm vco}^{\rm free}$ and vary $\omega_{\rm ref}$. First, we set frequency deviation $\left|\omega_e^{\rm free}\right| = 0$ and wait until the model reaches the locked state (since the pull-in range is infinite, the loop will lock eventually). Then we choose a sufficiently small frequency step $\Delta\omega > 0$. At the $k^{\rm th}$ step we abruptly change the carrier frequency by $(-1)^k(2k+1)\Delta\omega$ (i.e. the carrier frequency becomes $\omega_{\rm ref} = \omega_{\rm vco}^{\rm free} + (-1)^k(k+1)\Delta\omega$) and observe whether the corresponding transient process converges to a locked state without cycle slipping. We stop the procedure at $k = N$ when cycle slipping is detected during transient process. The desired frequency deviation ω_l is approximated as $N\Delta\omega < \omega_l \leq (N+1)\Delta\omega$.

Although in practice unstable equilibria of mathematical model (11) cannot be maintained, the lock-in definition admits unstable equilibria as a starting point for synchronization. To take this into account, at every step of the lock-in estimate one may start integration from vicinity of unstable equilibria (saddle) instead of stable one. Comparison of both approaches is shown in Fig. 4.

Note, that the transformation $x \to x/\tau_1$ does not affect the cycle slipping property of trajectories. Therefore, the lock-in range of (11) is a function of two parameters:

$$\omega_l = \omega_l(K_{\rm vco}, \tau_1, \tau_2) = \omega_l(K_{\rm vco}/\tau_1, \tau_2). \tag{14}$$

Thus, the estimate for model (11) described above can be compared with the lock-in range estimate in (Aleksandrov et al., 2016a,b) (see Fig. 3).

5. CONCLUSION

In this paper a modified QPSK Costas loop is studied. It is shown that the lock-in range estimation, taking into

[4] If necessary conditions for the averaging are satisfied (i.e. considered frequencies are sufficiently large) then complete synchronization for the mathematical model in the signal's phase space implies almost complete synchronization for the mathematical model in the signal space (Mitropolsky, 1967, p.88),(Kudrewicz and Wasowicz, 2007).

[5] Here and further upper index 's' denotes stable equilibria, and upper index 'u' denotes unstable equilibria.

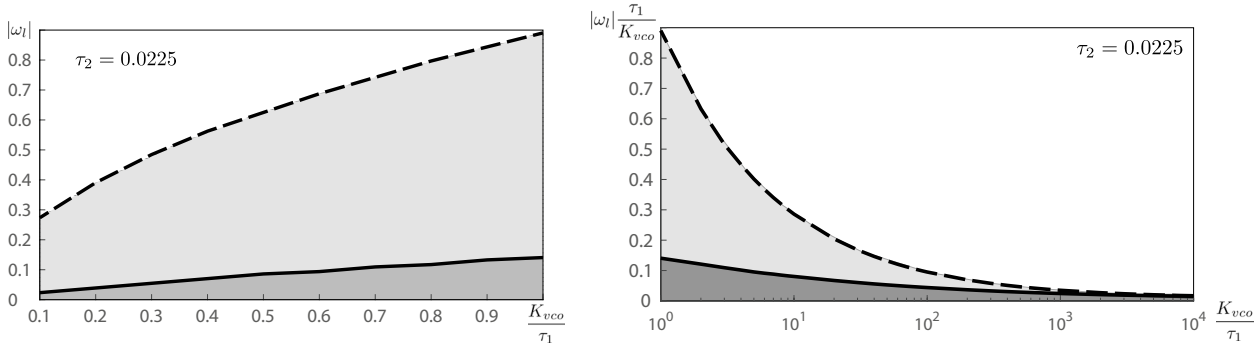

Fig. 3. Lock-in diagrams for modification of QPSK demodulator and active-PI loop filter. Here diagrams are given for fixed $\tau_2 = 0.0225$. Dashed line and light grey area on both pictures correspond to the estimate (Aleksandrov et al., 2016b), solid line and dark grey area - to the new estimate.

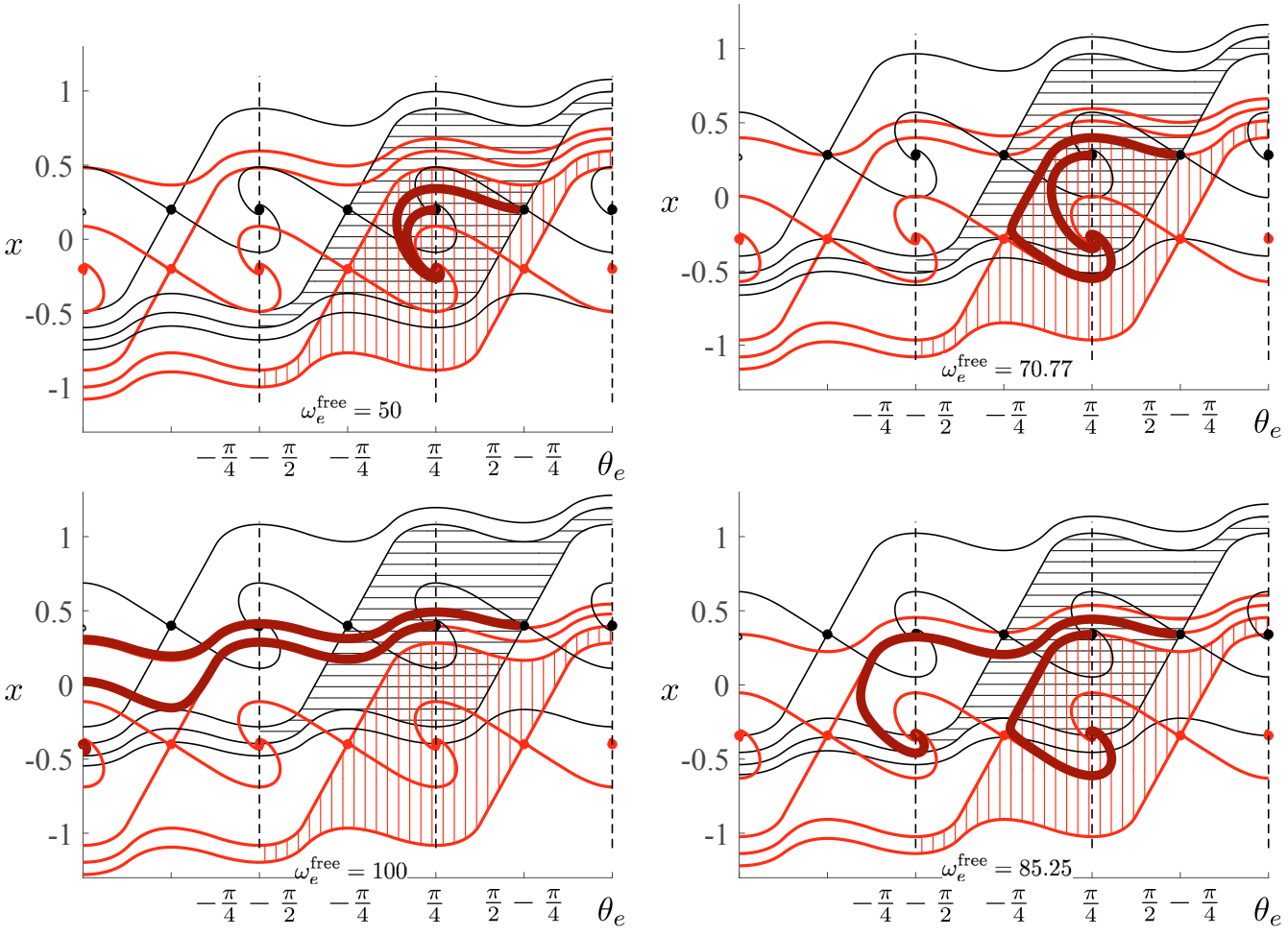

Fig. 4. Phase portraits for model (11) (active PI filter) with following parameters: $H(s) = \frac{1+s\tau_2}{s\tau_1}$, $\tau_1 = 0.0633$, $\tau_2 = 0.0225$, $K_{\text{vco}} = 250$, $v_e(\theta_e)$ defined by formula (5). Black color (thin curves) is for the model with positive $\omega_e^{\text{free}} = |\widetilde{\omega}|$. Red color (thick curves) is for the model with negative $\omega_e^{\text{free}} = -|\widetilde{\omega}|$. Equilibria are dots, separatrices pass in and out of the saddles equilibria, local lock-in domains are shaded (upper black horizontal lines are for $\omega_e^{\text{free}} > 0$, lower red vertical lines are for $\omega_e^{\text{free}} < 0$). Dark red (the thickest) curves start at the black equilibria after the abrupt change of $\omega_e^{\text{free}} \to -|\widetilde{\omega}|$. Left upper and lower subfigures correspond to $\omega_e^{\text{free}} < \omega_{\text{lock-in}}$ and $\omega_e^{\text{free}} > \omega_{\text{lock-in}}$, respectively. Right upper and lower subfigures correspond to the approximation of the lock-in range with respect to all locked states ($\omega_{\text{lock-in}} \approx 70.77$) and to the stable locked states only ($\omega_{\text{lock-in}} \approx 85.25$), respectively.

account unstable equilibria, gives much more conservative results (the lock-in range is much smaller). While in this article only second-order system is studied, higher order loop filter may be considered either numerically or using Lyapunov-like functions and frequency domain criterions (see, e.g. (Leonov and Kuznetsov, 2014)).

REFERENCES

Aleksandrov, K., Kuznetsov, N., Leonov, G., Neittaanmaki, N., Yuldashev, M., and Yuldashev, R. (2016a). Computation of the lock-in ranges of phase-locked loops with PI filter. *IFAC-PapersOnLine*, 49(14), 36–41. doi: 10.1016/j.ifacol.2016.07.971.

Aleksandrov, K., Kuznetsov, N., Leonov, G., Yuldashev, M., and Yuldashev, R. (2016b). Lock-in range of classical PLL with impulse signals and proportionally-integrating filter. *arXiv preprint arXiv:1603.09363*.

Alexandrov, K., Kuznetsov, N., Leonov, G., Neittaanmaki, P., and Seledzhi, S. (2015). Pull-in range of the classical {PLL} with impulse signals. *IFAC-PapersOnLine*, 48(1), 562 – 567. doi:10.1016/j.ifacol.2015.05.090.

Ascheid, G. and Meyr, H. (1982). Cycle slips in phase-locked loops: A tutorial survey. *Communications, IEEE Transactions on*, 30(10), 2228–2241.

Best, R.E. (2018). *Costas Loops: Theory, Design, and Simulation*. Springer International Publishing.

Best, R. (2007). *Phase-Locked Loops: Design, Simulation and Application*. McGraw-Hill, 6th edition.

Best, R., Kuznetsov, N., Leonov, G., Yuldashev, M., and Yuldashev, R. (2016). Tutorial on dynamic analysis of the Costas loop. *Annual Reviews in Control*, 42, 27–49. doi:10.1016/j.arcontrol.2016.08.003.

Bianchi, G., Kuznetsov, N., Leonov, G., Seledzhi, S., Yuldashev, M., and Yuldashev, R. (2016). Hidden oscillations in SPICE simulation of two-phase Costas loop with non-linear VCO. *IFAC-PapersOnLine*, 49(14), 45–50. doi:10.1016/j.ifacol.2016.07.973.

Bonnin, M., Corinto, F., and Gilli, M. (2014). Phase noise, and phase models: Recent developments, new insights and open problems. *Nonlinear Theory and Its Applications, IEICE*, 5(3), 365–378. doi:10.1587/nolta.5.365.

Ershova, O. and Leonov, G. (1983). Frequency estimates of the number of cycle slidings in phase control systems. *Avtomat. Remove Control*, 44(5), 600–607.

Gardner, F. (1966). *Phaselock techniques*. John Wiley & Sons, New York.

Kolumban, G. (2015). Software defined electronics: A revolutionary change in design and teaching paradigm of RF radio communications systems. *ICT Express*, 1(1), 44 – 54. doi:https://doi.org/10.1016/S2405-9595(15)30021-7.

Kudrewicz, J. and Wasowicz, S. (2007). *Equations of phase-locked loop. Dynamics on circle, torus and cylinder*. World Scientific.

Kuznetsov, N., Kuznetsova, O., Leonov, G., Yuldashev, M., and Yuldashev, R. (2017a). A short survey on nonlinear models of QPSK Costas loop. *IFAC-PapersOnLine*, 50(1), 6525 – 6533.

Kuznetsov, N., Leonov, G., Yuldashev, M., and Yuldashev, R. (2015). Rigorous mathematical definitions of the hold-in and pull-in ranges for phase-locked loops. *IFAC-PapersOnLine*, 48(11), 710–713. doi: 10.1016/j.ifacol.2015.09.272.

Kuznetsov, N., Leonov, G., Yuldashev, M., and Yuldashev, R. (2017b). Solution of the Gardner problem on the lock-in range of phase-locked loop. *ArXiv e-prints*. 1705.05013.

Ladvánszky, J. and Covács, B. (2018). Methods and apparatus for signal demodulation. Patent application P74032. Ericsson inc.

Ladvánszky, J. (2018). A costas loop variant for large noise. *Journal of Asian Scientific Research*, 8(3), 144–151.

Leonov, G. and Kuznetsov, N. (2014). *Nonlinear mathematical models of phase-locked loops. Stability and oscillations*. Cambridge Scientific Publishers.

Leonov, G., Kuznetsov, N., Yuldashev, M., and Yuldashev, R. (2015). Hold-in, pull-in, and lock-in ranges of PLL circuits: rigorous mathematical definitions and limitations of classical theory. *IEEE Transactions on Circuits and Systems–I: Regular Papers*, 62(10), 2454–2464. doi: 10.1109/TCSI.2015.2476295.

Margaris, N. (2004). *Theory of the Non-Linear Analog Phase Locked Loop*. Springer Verlag, New Jersey.

Matrosov, V.V., Mishchenko, M.A., and Shalfeev, V.D. (2013). Neuron-like dynamics of a phase-locked loop. *The European Physical Journal Special Topics*, 222(10), 2399–2405.

Mitropolsky, I.A. (1967). Averaging method in nonlinear mechanics. *International Journal of Non-Linear Mechanics*, 2(1), 69–96.

Piqueira, J. and Monteiro, L. (2003). Considering second-harmonic terms in the operation of the phase detector for second-order phase-locked loop. *IEEE Transactions On Circuits And Systems-I*, 50(6), 805–809.

Suarez, A. (2009). *Analysis and Design of Autonomous Microwave Circuits*. Wiley Series in Microwave and Optical Engineering. Wiley-IEEE Press.

Viterbi, A. (1966). *Principles of coherent communications*. McGraw-Hill, New York.